

## Molecular Tectonics: Grid and Porous Coordination Networks Based on Combinations of Iron Thiocyanate and Pyridyl Appended Derivatives of Tetrathiacalix[4]arene and Tetramercaptotetrathiacalix[4]arene

A. S. Ovsyannikov,<sup>a,c</sup> S. Ferlay,<sup>b</sup> S. E. Solovieva,<sup>a,c</sup> I. S. Antipin,<sup>a,c</sup> A. I. Konovalov,<sup>a</sup> N. Kyritsakas,<sup>b</sup> and M. W. Hosseini<sup>b</sup>

<sup>a</sup>Kazan Federal University, 420008 Kazan, Russian Federation

<sup>b</sup>Laboratory of Molecular Tectonics, University of Strasbourg, UMR UDS-CNRS 7140, Institut le Bel, F-67000 Strasbourg, France

<sup>c</sup>A.E. Arbuzov Institute of Organic and Physical Chemistry of Kazan Scientific Center of Russian Academy of Sciences, 420088 Kazan, Russian Federation

@Corresponding author E-mail: [osaalex2007@rambler.ru](mailto:osaalex2007@rambler.ru)

*The combination of three pyridyl appended tetrathiacalix[4]arene (TCA) and tetramercaptotetrathiacalix[4]arene (TMTCa) derivatives in 1,3-alternate imposed conformation behaving as neutral tectons with octahedral Fe<sup>II</sup>(NCS)<sub>2</sub> complex as a metallatecton, leads to the formation of new coordination networks. Whereas the tecton 4, a tetrasubstituted TCA derivative (pyridyl in ortho position), leads to a 2D grid-like network, for the other two tectons 5 and 6, the formation of 3D diamond-like architectures is observed.*

**Keywords:** Molecular tectonics, coordination polymer, tetrathiacalix[4]arene, tetramercaptotetrathiacalix[4]arene, iron(II) thiocyanate.

## Молекулярная тектоника: создание решётчатых и пористых координационных сеток на основе взаимодействия тиоцианата железа с пиридинными производными тетратиакаликс[4]арена и тетрамеркаптотетратиакаликс[4]арена

A. S. Овсянников,<sup>a</sup> С. Ферлэй,<sup>b</sup> С. Е. Соловьёва,<sup>a,c</sup> И. С. Антипин,<sup>a,c</sup> А. И. Коновалов,<sup>a</sup> Н. Киритсакас,<sup>b</sup> М. В. Хоссейни<sup>b</sup>

<sup>a</sup>Казанский федеральный университет, 420008 Казань, Россия

<sup>b</sup>Лаборатория молекулярной тектоники, Университет Страсбурга, F-67000 Страсбург, Франция

<sup>c</sup>Институт органической и физической химии им. А.Е. Арбузова КазНЦ РАН, 420088 Казань, Россия

@E-mail: [osaalex2007@rambler.ru](mailto:osaalex2007@rambler.ru)

*Взаимодействие пиридинных производных тетратиакаликс[4]арена и тетрамеркаптотетратиакаликс[4]арена в конформации 1,3-альтернат с тиоцианатом железа(II) привело к образованию 2D (структура решётки) и 3D пористых координационных сеток (алмазоподобная структура) в кристаллической фазе.*

**Ключевые слова:** Молекулярная тектоника, координационный полимер, тетратиакаликс[4]арен, тетрамеркаптотетратиакаликс[4]арен, тиоцианат железа(II).

## Introduction

Molecular tectonics<sup>[1]</sup> is a powerful approach for the design of molecular networks<sup>[2]</sup> in the crystalline phase and on surfaces.<sup>[3]</sup> This approach, taking place under self-assembly conditions, is based on combinations of complementary tectons<sup>[4]</sup> capable of mutual bridging through molecular recognition events. Among different types of molecular networks based on a variety of recognition patterns such as van der Waals contacts, H-bonding,  $\pi$ - $\pi$  or M-M interactions, coordination bonding, the latter has attracted considerable attention over the last two decades.<sup>[5]</sup>

Calix[4]arene (CA) **1**,<sup>[6]</sup> tetrathiacalix[4]arene (TCA) **2**,<sup>[7]</sup> for which all four CH<sub>2</sub> moieties are replaced by four S atoms, tetramercapto-calix[4]arene (TMCA)<sup>[8]</sup> and tetramercaptotetrathiacalix[4]arene (TMTCA) **3**<sup>[9]</sup> for which the OH phenolic groups are replaced by SH moieties (Figure 1) in their *1,3*-alternate (*1,3*-A) conformation are interesting macrocyclic backbone for the design of coordinating tectons. Indeed, this conformer, displaying a S<sub>4</sub> rotoinversion axis, may be appended with four coordinating groups. The latter, oriented in a divergent fashion (two above and two below the main plane of the macrocyclic unit) may interconnect consecutive metal centres offering free coordination sites leading thus to periodic metal-organic networks.

Based on calix[4]arene derivatives blocked in its *1,3*-A conformation, different coordination polymers,<sup>[10]</sup> such as

coordination networks<sup>[11]</sup> or metal organic frameworks<sup>[12]</sup> have been reported. For example, using a CA derivative bearing four nitrile groups in the upper rim, a 1D coordination network was generated in the crystalline phase in the presence of Ag<sup>+</sup> cation.<sup>[13]</sup> The formation of extended assemblies resulting from combinations of CA based tectons bearing carboxylate groups with Ag<sup>II</sup><sup>[14]</sup> or Cu<sup>II</sup>, Zn<sup>II</sup>, Co<sup>II</sup> or Cd<sup>II</sup> cations has been also described.<sup>[15]</sup> The combination of a CA bearing pyridyl moieties with Cu<sup>II</sup> cation was found to lead to the formation of extended architectures.<sup>[16]</sup>

Several periodic infinite silver or mercury coordination networks based on TCA derivatives in *1,3*-A conformation bearing four nitrile,<sup>[17]</sup> pyridyl,<sup>[18]</sup> carboxylate<sup>[19]</sup> or benzonitrile groups<sup>[20]</sup> have been described. In some cases, the combination of TCA and silver(I)<sup>[21]</sup> or copper(I)<sup>[22]</sup> cations leads to the formation of extended metal-organic structures for which only S-atoms are involved in coordination of the metal cation. Furthermore, combinations of TCA derivatives bearing carboxylate groups with Co<sup>II</sup>, Cd<sup>II</sup> or Mn<sup>II</sup> cations and auxiliary ligands generate infinite architectures.<sup>[23]</sup> Dealing with TMTCA in *1,3*-A conformation, only few examples of coordination networks resulting from combinations of its pyridyl appended derivatives with Hg<sup>II</sup>,<sup>[24]</sup> Fe<sup>II</sup>, Co<sup>II</sup> or Ag<sup>I</sup><sup>[25]</sup> cations have been reported.

Here, we report on formation of 2-D (grid type) and 3-D (diamond type) coordination networks based on combinations of TCA (**4**) and (**5**) and TMTCA (**6**) in *1,3*-A

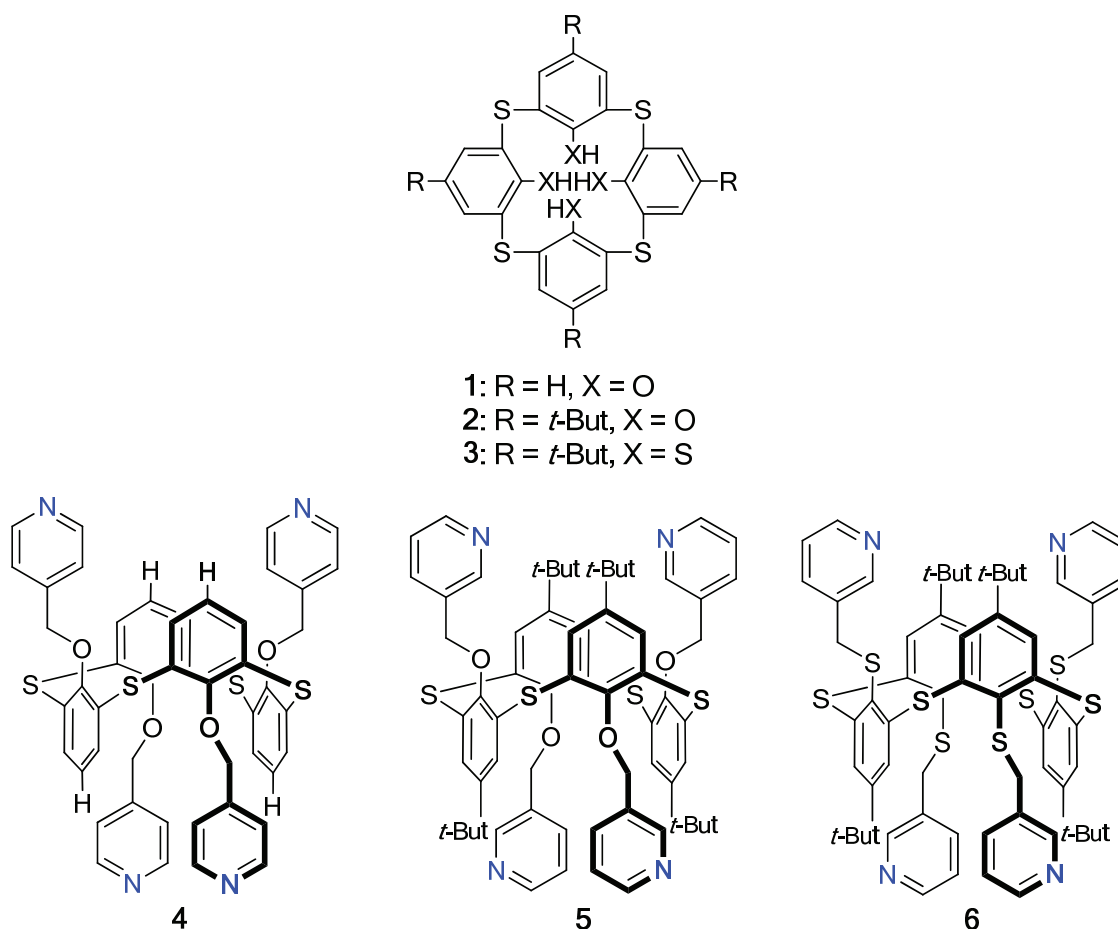


**Figure 1.** Tetrathia- and tetrathiatetramercapto-calix[4]arene precursors **1**, **2** and **3** and tetrapyridyl appended tectons **4** (*para*-), **5** (*meta*-) and **6** (*meta*-) in *1,3*-A conformation.

conformation based neutral tectons with  $\text{Fe}^{\text{II}}(\text{NCS})_2$  species used as a 4-connecting metallatecton.

## Experimental

All reagents were purchased from commercial sources and used without further purification. The synthesis of **4**<sup>[18a]</sup> (25,26,27,28-tetra[(4-pyridylmethyl)oxy]-5,11,17,23-tetra-*tert*-butyl-2,8,14,20-tetrathiacalix[4]arene), **5**<sup>[18b]</sup> (25,26,27,28-(25,26,27,28-tetra[(4-pyridylmethyl)oxy]-5,11,17,23-tetra-*tert*-butyl-2,8,14,20-tetrathiacalix[4]arene) and **6**<sup>[19]</sup> (25,26,27,28-tetra[(3-pyridylmethyl)thio]-5,11,17,23-tetra-*tert*-butyl-2,8,14,20-tetrathiacalix[4]arene) in *1,3-A* conformation have already been reported.  $\text{Fe}^{\text{II}}(\text{NCS})_2(\text{Py})_4$  was prepared following a described procedure.<sup>[26]</sup>

Elemental analyses were performed by the Service de Microanalyses de la Fédération de Recherche Chimie, Université de Strasbourg, Strasbourg, France.

Data for X-Ray analysis were collected at 173(2) K on a Bruker APEX8 CCD Diffractometer equipped with an Oxford Cryosystem liquid  $\text{N}_2$  device, using graphite-monochromated Mo-K $\alpha$  ( $\lambda = 0.71073 \text{ \AA}$ ) radiation. For all structures, diffraction data were corrected for absorption. Structures were solved using SHELXS-97 and refined by full matrix least-squares on  $F^2$  using SHELXL-97. The hydrogen atoms were introduced at calculated positions and not refined (riding model).<sup>[27]</sup> They can be obtained free of charge from the Cambridge Crystallographic Data Centre via [www.ccdc.cam.ac.uk/datarequest/cif](http://www.ccdc.cam.ac.uk/datarequest/cif). CCDC: 1411457-1411459.

Powder diffraction studies (PXRD) diagrams were collected on a Bruker D8 diffractometer using monochromatic Cu-K $\alpha$  radiation with a scanning range between 3.8 and 40° using a scan step size of 2°/mn.

As it was already demonstrated and currently admitted, for all the compounds, discrepancies in intensity between the observed and simulated patterns are due to preferential orientations of the microcrystalline powders.

## Crystallisation Conditions

**4-Fe(NCS)<sub>2</sub>**: In a crystallisation tube (4 mm diameter, 15 cm height), a solution of compound **4** (5 mg, 5.8 mmol) in degassed  $\text{CHCl}_3$  (1 mL) was layered with a degassed  $\text{CHCl}_3/\text{iso-PrOH}$  (1/1) mixture (1 mL). A solution of  $\text{Fe}(\text{NCS})_2(\text{Py})_4$  (2.8 mg, 5.8 mmol) in degassed MeOH (1 mL) was carefully added. Slow diffusion at room temperature produced red crystals suitable for X-ray diffraction studies after several days. Formula:  $(\text{C}_{49}\text{H}_{36}\text{N}_4\text{O}_4\text{S}_4\text{Fe}(\text{NCS})_2)_2 \cdot 3(\text{CHCl}_3)$  Anal. Calcd.: C, 52.15%; H, 3.16%; N, 6.76%; Found: C, 52.32%; H, 3.24%; N, 6.80%.

**5-Fe(NCS)<sub>2</sub>**: A solution of compound **5** (5 mg, 4.6 mmol) in degassed  $\text{CHCl}_3$  (1 mL) was mixed with a solution of  $\text{Fe}(\text{NCS})_2(\text{Py})_4$  (2.2 mg, 4.6 mmol) in degassed MeOH (1 mL) in a flask. After two days, the flask was placed in another flask containing ether. Slow vapour diffusion at room temperature produced after several days red crystals suitable for X-ray diffraction studies. Formula:  $\text{C}_{64}\text{H}_{68}\text{N}_4\text{O}_4\text{S}_4\text{Fe}(\text{NCS})_2 \cdot 5(\text{CHCl}_3)$  Anal. Calcd.: C, 45.99%; H, 3.97%; N, 4.53%; Found: C, 46.25%; H, 4.03%; N, 4.62%.

**6-Fe(NCS)<sub>2</sub>**: A solution of compound **6** (5 mg, 4.3 mmol) in degassed  $\text{CHCl}_3$  (1 mL) was mixed with a solution of  $\text{Fe}(\text{NCS})_2(\text{Py})_4$  (2.2 mg, 4.3 mmol) in degassed MeOH (1 mL) in a flask. After two days the crystallization flask was placed in another flask containing ether. Slow vapour diffusion at room temperature produced after several days red crystals suitable for X-ray diffraction studies. Formula:  $\text{C}_{64}\text{H}_{68}\text{N}_4\text{S}_8\text{Fe}(\text{NCS})_2 \cdot 2(\text{H}_2\text{O})$  Anal. Calcd.: C, 57.63%; H, 5.44%; N, 6.30%; Found: C, 57.82%; H, 5.51%; N, 6.35%.

## Results and Discussion

Although tectons **4**, **5** and **6** offer four divergently oriented pyridyl moieties as coordinating sites and thus should behave as a 4-connecting building block, owing to their flexibility resulting from the interconnection of the coordinating sites to the backbone, they can adopt different orientations of the binding sites. Consequently, their combination with octahedral  $\text{Fe}^{\text{II}}(\text{NCS})_2$  complex behaving as a 4-connecting node since the two apical position of the octahedron are occupied by the two  $\text{NCS}^-$  ligands, may lead to different architectures displaying diverse connectivity and thus dimensionalities.

The slow diffusion of a MeOH solution of  $\text{Fe}^{\text{II}}(\text{NCS})_2(\text{Py})_4$  through a 1/1  $\text{CHCl}_3/\text{iso-PrOH}$  mixture as buffer into a  $\text{CHCl}_3$  solution of tecton **4** afforded red single crystals (**4-Fe(NCS)<sub>2</sub>**, formula  $(\text{C}_{49}\text{H}_{36}\text{N}_4\text{O}_4\text{S}_4\text{Fe}(\text{NCS})_2)_2 \cdot 3\text{CHCl}_3$ ) (see Experimental part), containing the tecton **4**,  $\text{Fe}(\text{NCS})_2$  complex and  $\text{CHCl}_3$  solvent molecules. Single crystals of **5-Fe(NCS)<sub>2</sub>** ( $\text{C}_{64}\text{H}_{68}\text{N}_4\text{O}_4\text{S}_4\text{Fe}(\text{NCS})_2 \cdot 5\text{CHCl}_3$ ) and **6-Fe(NCS)<sub>2</sub>** ( $\text{C}_{64}\text{H}_{68}\text{N}_4\text{S}_8\text{Fe}(\text{NCS})_2 \cdot 2\text{H}_2\text{O}$ ) have been obtained upon slow ether vapour diffusion into a  $\text{CHCl}_3/\text{MeOH}$  solution containing either compound **5** or **6** and  $\text{Fe}(\text{NCS})_2(\text{Py})_4$  complex.

Structural investigations by X-ray diffraction on single crystals revealed that in all three cases, the metal/tecton ratio is 1/1. In the case of **4** (*para*-pyridyl), a 2D network is observed, whereas for the *meta*-pyridyl connected tectons **5** and **6**, 3D architectures are obtained. In all three cases, the formation of networks results from bridging of consecutive organic tectons by  $\text{Fe}^{\text{II}}(\text{NCS})_2$  behaving as a 4-connecting node. The geometry around the  $\text{Fe}^{\text{II}}$  centre is a deformed octahedron and its coordination sphere is composed of 6 N atoms (2 from  $\text{NCS}$  and 4 from pyridyl ligands belonging to consecutive tectons). Since bond distances for tectons **4**, **5** and **6** are similar to those previously observed<sup>[18,24]</sup> they are not discussed here. The detailed description of the three coordination networks is given below.

**4-Fe(NCS)<sub>2</sub>** crystallises in a *monoclinic* system ( $P2(1)/n$  space group) and is composed of neutral ligand **4**, neutral  $\text{Fe}(\text{NCS})_2$  complex and  $\text{CHCl}_3$  solvent molecules. Overall, the crystal is formed by packing of 2D grid type networks. The 2D connectivity results from the bridging of consecutive tectons **4**, acting as a deformed tetradentate rectangular unit, by the metallatecton  $\text{Fe}(\text{NCS})_2$  offering four free coordination sites occupying the apices of a square. The thiocyanate anions, located in *trans* disposition within the octahedral coordination sphere of the iron, are not involved in the connectivity pattern (Figure 2).  $\text{Fe}^{\text{II}}$  adopts a slightly deformed octahedral geometry. Fe-N bond distances vary between 2.106(3) and 2.318(3) Å. N-Fe-N angles vary between 88.43(10) and 92.88(11)° (*cis*) and 175.44(10) and 177.66(12)° (*trans*). For precise values see Table 1.

The 2D grid type arrays, lying in the *xOz* plane, are packed in a parallel mode along the *b* axis. The  $\text{CHCl}_3$  molecules are located between planes with no specific interactions with consecutive networks.

The purity of the **4-Fe(NCS)<sub>2</sub>** phase was established by PXRD on microcrystalline powder which revealed a good match between the observed and simulated patterns from the XRD data (Figure 3).

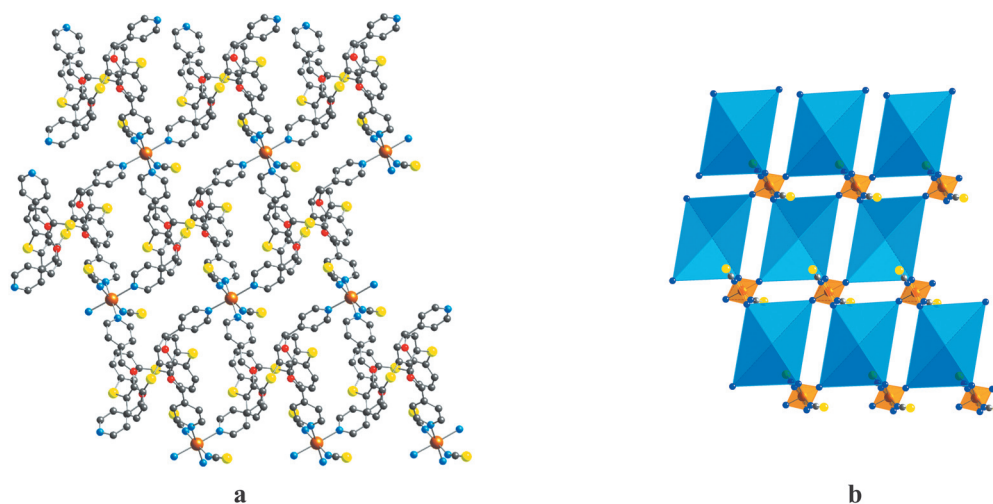


**Figure 2.** A portion of the crystal structure of  $4\text{-Fe}(\text{NCS})_2$  in the  $xOz$  plane (a) and the corresponding polyhedral representation (b) (tecton **4** in blue and  $\text{Fe}^{\text{II}}$  in brown). H atoms and  $\text{CHCl}_3$  molecules are omitted for clarity. For bond distances and angles see the text.

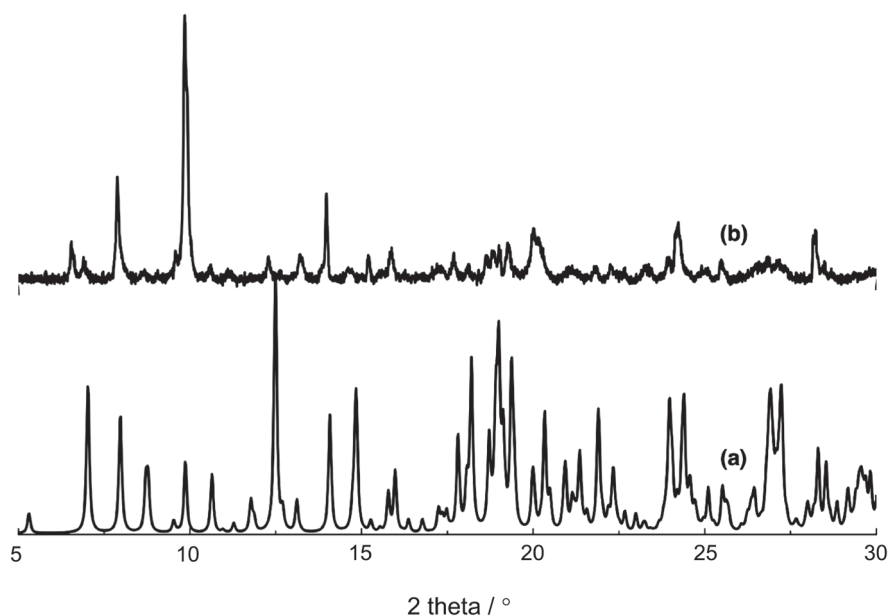


**Figure 3.** Comparison of the simulated (a) and recorded (b) PXRD patterns for  $4\text{-Fe}(\text{NCS})_2$ . Discrepancies in intensity between the observed and simulated patterns are due to preferential orientations of the microcrystalline powders.

$5\text{-Fe}(\text{NCS})_2$  crystallises in a *monoclinic* system ( $C2/c$  space group) and is also composed of neutral tecton **5**, neutral  $\text{Fe}(\text{NCS})_2$  complex and  $\text{CHCl}_3$  solvent molecules. Overall, the crystal is formed by a pseudo diamond-like 3D network. The 3D connectivity results from the bridging of tectons **5**, behaving as a deformed tetradentate tetrahedral connector, by  $\text{Fe}^{\text{II}}$  centres acting as a 4-connecting node with the free coordination sites located in the basal plane. Again, the two thiocyanate anions occupy the two apical positions of the octahedron. The combination of the tecton **5**, offering a tetrahedral disposition of the pyridyl coordinating sites, with the metallatecton  $\text{Fe}(\text{NCS})_2$ , behaving as a 4-connecting square planar node, leads to the formation of a diamond-like 3D architecture (Figure 4). For  $\text{Fe}^{\text{II}}$  centre, Fe-N bond distances are 2.121(7), 2.227(6) and 2.229(6) Å. N-Fe-N angles for the slightly deformed octahedral environment around Fe

vary between 85.0(2) and 95.0(2) $^\circ$  (*cis*) and 179.998(1) and 180.0(3) (*trans*). For detailed values see Table 1.

The  $\text{CHCl}_3$  solvent molecules are located within the channels formed along the  $c$  axes. No specific interactions with the formed network could be spotted. Due to the instability of crystals when exposed to air, the purity of the microcrystalline powder could not be established by PXRD.

$6\text{-Fe}(\text{NCS})_2$  crystallises in the *monoclinic* system (space group  $C2/c$ ). The crystal is composed of neutral tecton **6**,  $\text{Fe}(\text{NCS})_2$  complex and water molecules. The overall structure is again a pseudo diamond-like network. The 3D connectivity of the architecture results from the bridging of consecutive tectons **6**, acting as a deformed tetradentate tetrahedral unit as in the case of **5** discussed above, by  $\text{Fe}(\text{NCS})_2$  behaving as a 4-connecting node. However, in marked contrast with the two previous cases presented above, the network is

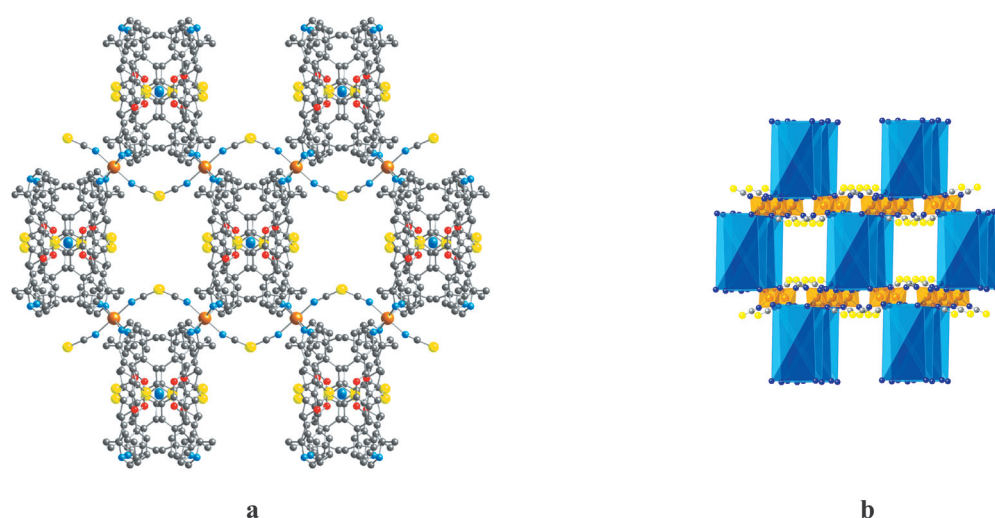


**Figure 4.** A portion of the crystal structure of the 3D diamond type architecture  $5\text{-Fe(NCS)}_2$  (a) and its polyhedral representation (b) (tecton **5** in blue,  $\text{Fe}^{\text{II}}$  in brown). H atoms and  $\text{CHCl}_3$  molecules are omitted for clarity. For bond distances and angles see the text.

composed of two types of octahedral  $\text{Fe}^{\text{II}}$  centres. For one of the positional isomer, as in the case of **4** and **5**, the two thiocyanate anions occupy the two apical positions (*trans* configuration), whereas for the other one the two  $\text{NCS}^-$  are in *cis* configuration. The 3D architecture may be described as resulting from bridging of consecutive tectons **6** displaying four pyridyl units as monodentate coordinating sites occupying the apices of a deformed tetrahedron by 4-connecting metallatectons  $\text{Fe(NCS)}_2$  (Fe SP) with square planar disposition of the free coordination sites  $\text{Fe(NCS)}_2$ , and  $\text{Fe(NCS)}_2$

(Fe T) displaying also four free coordination site but occupying the apices of a deformed tetrahedron (Figure 5). Fe-N bond distances and N-Fe-N angles for  $\text{Fe}^{\text{II}}$  adopting a slightly deformed octahedral environment vary between 2.106(3) and 2.318(3) Å and between 88.43(10) and 92.88(11)° (*cis*) and a 175.44(10) and 177.66(12)° (*trans*) respectively. For detailed values see Table 1.

The  $\text{H}_2\text{O}$  molecules are located within channels along the *a* axes. They form dimeric species with O-O distances of 2.834(3) Å.

**Table 1.** Main characteristics (distances and angles) for  $4\text{-Fe(NCS)}_2$ ,  $5\text{-Fe(NCS)}_2$  and  $6\text{-Fe(NCS)}_2$ . For definition of SP and T see text.

	$4\text{-Fe(NCS)}_2$	$5\text{-Fe(NCS)}_2$	$6\text{-Fe(NCS)}_2$	
			Fe SP	Fe T
$d(\text{Fe-N}_{\text{py}}), \text{Å}$	2.106(3)			
	2.114(3)			
	2.298(3)	2.227(6)	2.269(7)	2.206(9)
	2.318(3)	2.229(6)	2.272(6)	
$d(\text{Fe-N}_{\text{NCS}}), \text{Å}$	2.224(3)		2.108(8)	2.103(12)
	2.231(3)	2.121(7)		
$\angle (\text{N}_{\text{py}}\text{-Fe-N}_{\text{py}}), ^\circ$	88.43(10)			
	89.87(10)	85.0(2)		
	90.50(10)	95.0(2)	86.4(2) 93.6(2) 180.0(5)	175.7(5)
	91.27(10)	180.0(3)		
	175.44(10)			
$\angle (\text{N}_{\text{py}}\text{-Fe-N}_{\text{NCS}}), ^\circ$	178.61(10)			
	86.35(11)			
	89.11(11)			
	89.45(11)	89.2(2)	89.0(3) 89.4(3)	92.3(4)
	89.70(11)	89.9(2)	90.6(3)	91.4(4)
	90.04(11)	90.1(2)	91.0(3)	
$\angle (\text{N}_{\text{NCS}}\text{-Fe-N}_{\text{NCS}}), ^\circ$	91.11(11)	90.8(2)		
	91.32(11)			
	92.88(11)			
	177.66(12)	179.998(1)	179.998(2)	59.4(7)

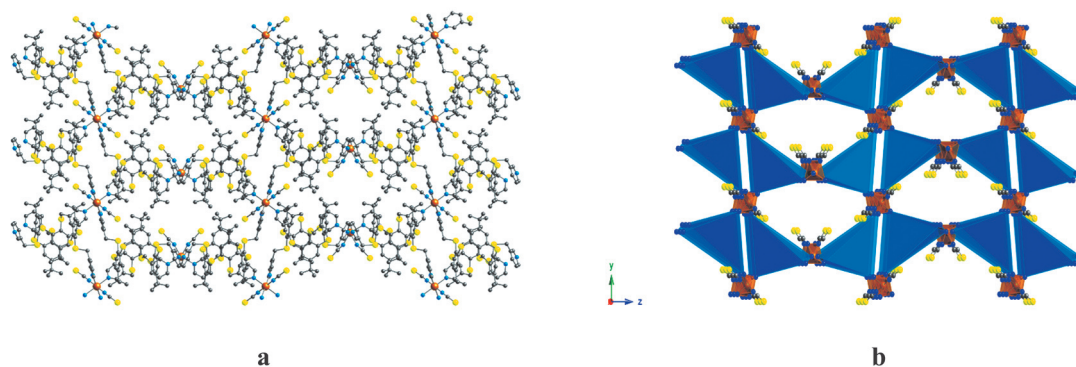


**Figure 5.** A portion of the crystal structure of the diamond type 3D network  $6\text{-Fe(NCS)}_2$  (a) and its polyhedral representation (b) (tecton **6** in blue and  $\text{Fe}^{\text{II}}$  in brown). H atoms and  $\text{H}_2\text{O}$  molecules are omitted for clarity. For bond distances and angles see the text.

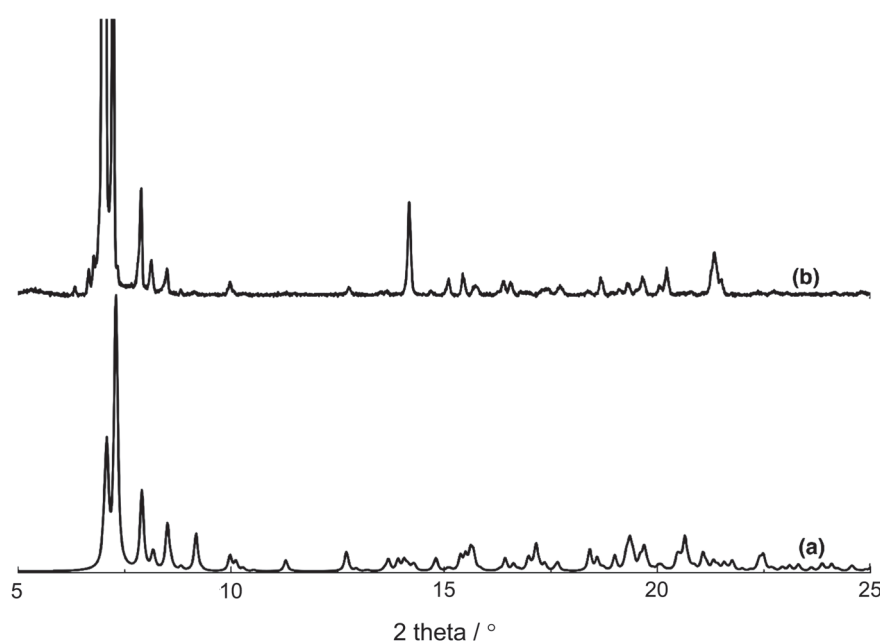


**Figure 6.** Comparison of the simulated (a) and recorded (b) PXRD patterns for  $6\text{-Fe(NCS)}_2$ . Discrepancies in intensity between the observed and simulated patterns are due to preferential orientations of the microcrystalline powders.

The purity of the  $6\text{-Fe(NCS)}_2$  phase was established by PXRD on microcrystalline powder which revealed a good match between the observed and simulated patterns from the XRD data (Figure 6).

## Conclusion

Tetrasubstituted TCA and TMTCA derivatives in *1,3-A* conformation equipped with four pyridyl monodentate coordinating sites **4** (4-pyridyl), **5** and **6** (3-pyridyl) respectively behave as 4-connecting coordinating tectons. Indeed, their combinations with  $\text{Fe}^{\text{II}}(\text{NCS})_2$  neutral metallatecton also behaving as a 4-connecting node lead to the formation of extended iron coordination networks. The nature of the periodic architectures (2D grid type or 3D diamond like) in the crystalline phase is governed by different parameters controlling the connectivity mode

between the organic coordinating tectons (**4**, **5** and **6**) and the metallatecton  $\text{Fe}(\text{NCS})_2$  such as (i) the position of the N atom on the pyridyl coordinating unit (*para* for **4** and *meta* for **5** and **6**), (ii) the presence or absence of bulky groups (H for **4** and *tert*-But for **5** and **6**) at the upper rim of the calix backbone, (iii) the presence of O (tectons **4** and **5**) or S (tecton **6**) atoms as junctions between appended groups and the macrocyclic ring (TCA or TMTCA).

Interestingly, for tecton **4** it seems that the orientation of the coordinating groups (4-pyridyl), together with the absence of bulky *tert*-But groups favour the formation of grid-like coordination networks when combined with  $\text{Fe}(\text{NCS})_2$ . The presence of bulky *tert*-But groups in **5** and **6**, increasing the distances between the coordinating groups, and the use of the *meta* position on the pyridyl ring seems to favour the formation of 3D diamond-like coordination networks. Moreover, comparing the crystal structures of coordination polymers constructed by using analogous

3-pyridyl containing tectons based on TCA and TMTCA one may conclude that the nature of ether junction (O or S atoms) influences on the geometry of self-assembly pattern but doesn't change the dimensionality of coordination polymers (3D).

**Acknowledgments.** This work has been supported by Russian Scientific Foundation (grant N 15-13-30006). We thank the University of Strasbourg, the Institut Universitaire de France (IUF) and icFRC for X-ray experiments and microanalysis.

## References

- (a) Mann S. *Nature* **1993**, *365*, 499; (b) Hosseini M.W. *Acc. Chem. Res.* **2005**, *38*, 313.
- Hosseini M.W. *CrystEngComm* **2004**, *6*, 318.
- (a) Surin M., Samori P., Jouaiti A., Kyritsakas N., Hosseini M.W. *Angew. Chem. Int. Ed.* **2007**, *46*, 245; (b) El Garah M., Ciesielski A., Marets N., Bulach V., Hosseini M.W., Samori P. *Chem. Commun.* **2014**, *50*, 12250; (c) El Garah M., Marets N., Mauro M., Aliprandi A., Bonacchi S., De Cola L., Ciesielski A., Bulach V., Hosseini M.W., Samori P. *J. Am. Chem. Soc.* **2015**, *137*, 8450.
- (a) Simard M., Su D., Wuest J.D. *J. Am. Chem. Soc.* **1991**, *113*, 4696; (b) Hosseini M.W. *Chem. Commun.* **2005**, 5825.
- (a) Abrahams B.F., Hoskins B.F., Robson R. *J. Am. Chem. Soc.* **1991**, *113*, 3606; (b) Batten S.R., Robson R. *Angew. Chem. Int. Ed.* **1998**, *37*, 1460; (c) Blake A.J., Champness N.R., Hubberstey P., Li W.-S., Withersby M.A., Schröder M. *Coord. Chem. Rev.* **1999**, *193*, 117; (d) Moulton B., Zaworotko M.J. *Chem. Rev.* **2001**, *101*, 1629; (e) Janiak C. *Dalton Trans.* **2003**, 2781; (f) Carlucci L., Ciani G., Proserpio D.M. *Coord. Chem. Rev.* **2003**, *246*, 247; (g) Kitagawa S., Kitaura R., Noro S. *Angew. Chem. Int. Ed.* **2004**, *43*, 2334; (h) Férey G., Mellot-Draznieks C., Serre C., Millange F. *Acc. Chem. Res.* **2005**, *38*, 218; (i) Bradshaw D., Claridge J.B., Cussen E.J., Prior T.J., Rosseinsky M.J. *Acc. Chem. Res.* **2005**, *38*, 273; (j) Kitagawa S., Uemura K. *Chem. Soc. Rev.* **2005**, *34*, 109; (k) MasPOCH D., Ruiz-Molina D., Veciana J. *Chem. Soc. Rev.* **2007**, *36*, 770; (l) Long J.R., Yaghi O.M. *Chem. Soc. Rev.* **2009**, *38*, 1213; (m) Janiak C., Vieth J.L. *New J. Chem.* **2010**, *34*, 2366; (n) *Chem. Soc. Rev.* **2009**, *38*, themed issue on metal-organic frameworks; (o) Leong W.L., Vittal J.J. *Chem. Rev.* **2011**, *111*, 688; (p) *Chem. Rev.* **2012**, *112*, Metal-Organic Frameworks, special issue.
- (a) Gutsche C.D. *Calixarenes Revisited (Monographs in Supramolecular Chemistry)*, Vol. 6, The Royal Society of Chemistry, Cambridge, **1998**; (b) Asfari Z., Böhmer V., Harrowfield J., Vicens J. In: *Calixarenes 2001* (Asfari Z., Böhmer V., Harrowfield J., Vicens J., Eds.) Kluwer Academic, Dordrecht, **2001**.
- (a) Kumagai H., Hasegawa M., Miyanari S., Sugawa Y., Sato Y., Hori T., Ueda S., Kamiyama H., Miyano S. *Tetrahedron Lett.* **1997**, *38*, 3971; (b) Akdas H., Bringel L., Graf E., Hosseini M.W., Mislin G., Pansanel J., De Cian A., Fischer J. *Tetrahedron Lett.* **1998**, *39*, 2311.
- Hosseini M.W. In: *Calixarenes 2001* (Asfari Z., Böhmer V., Harrowfield J., Vicens J., Eds.) Kluwer Academic, Dordrecht, **2001**, 110 pp.
- Rao P., Hosseini M.W., Cian A.D., Fischer J. *Chem. Commun.* **1999**, 2169.
- (a) Abrahams B.F., Hoskins B.F., Robson R. *J. Am. Chem. Soc.* **1991**, *113*, 3606; (b) Batten S.R., Robson R. *Angew. Chem. Int. Ed.* **1998**, *37*, 1460.
- (a) Kaes C., Hosseini M.W. *NATO ASI Series* (Viciano J., Ed.) **1998**, *C518*, 53; (b) Hosseini M.W. *NATO ASI Series* (Tsoucaris G., Ed.) **1998**, *C519*, 209; (c) Hosseini M.W. *NATO ASI Series* (Braga D., Orpen G., Eds.) **1999**, *C538*, 181.
- (a) Yaghi O.M., Li H., Davis C., Richardson D., Groy T.L. *Acc. Chem. Res.* **1998**, *31*, 474; (b) Eddaoudi M., Moler D.B., Li H., Chen B., Reineke T.M., O'Keeffe M., Yaghi O.M. *Acc. Chem. Res.* **2001**, *34*, 319.
- Mislin G., Graf E., Hosseini M.W., De Cian A., Kyritsakas N., Fischer J. *Chem. Commun.* **1998**, 2545.
- Park K.-M., Lee E., Park C.S., Lee S.S. *Inorg. Chem.* **2011**, *50*, 12085.
- (a) Liu Y.-J., Huang J.-S., Chui S. S.-Y., Li C.-H., Zuo J.-L., Zhu N., Che C.-M. *Inorg. Chem.* **2008**, *47*, 11514; (b) Bew S.P., Burrows A.D., Düren T., Mahon M.F., Moghadam P.Z., Sebestyen V.M., Thurston S. *Chem. Commun.* **2012**, 4824; (c) Liu Y.-Y., Chen C., Ma J.-F., Yang J. *CrystEngComm* **2012**, *14*, 6201; (d) Redshaw C., Rowe O., Elsegood M.R.J., Horsburgh L., Teat S.J. *Cryst. Growth Des.* **2014**, *14*, 270; (e) Tsybmal L.V., Lampeka Y.D., Boyko V.I., Kalchenko V.I., Shishkina S.V., Shishkin O.V. *CrystEngComm* **2014**, *16*, 3707.
- (a) Olguín J., Gómez-Vidales V., Muñoz E., Toscano R.A., Castillo I. *Inorg. Chem. Commun.* **2006**, *9*, 1096-1098; (b) Olguín J., Gómez-Vidales V., Hernández-Ortega S., Toscano R.A., Muñoz E., Castillo I. *Supramol. Chem.* **2009**, *21*, 502.
- Kozlova M.N., Ferlay S., Solovieva S.E., Antipin I.S., Konovalov A.I., Kyritsakas N., Hosseini M.W. *Dalton Trans.* **2007**, 5126.
- (a) Ovsyannikov A., Ferlay S., Solovieva S.E., Antipin I.S., Konovalov A.I., Kyritsakas N., Hosseini M.W. *Dalton* **2013**, *42*, 9946; (b) Ovsyannikov A., Lang M.N., Ferlay S., Solovieva S.E., Antipin I.S., Konovalov A.I., Kyritsakas N., Hosseini M.W. *Dalton Trans.* **2013**, *42*, 116.
- Akdas H., Graf E., Hosseini M.W., De Cian A., Harrowfield J.M. *Chem. Commun.* **2000**, 2219.
- Kozlova M.N., Ferlay S., Kyritsakas N., Hosseini M.W., Solovieva S.E., Antipin I.S., Konovalov A.I. *Chem. Commun.* **2009**, 2514.
- Sykora J., Himl M., Stobor I., Cisarova I., Lhotak P. *Tetrahedron* **2007**, *63*, 2244.
- Bi Y., Liao W., Wang X., Deng R., Zhang H. *Eur. J. Inorg. Chem.* **2009**, 4989.
- (a) Kim K., Park S., Park K.-M., Lee S.S. *Cryst. Growth Des.* **2011**, *11*, 4059; (b) Liu M., Liao W. *Chem. Commun.* **2012**, 5727; (c) Zhang Z., Drapailo A., Matvieiev Y., Wojtas L., Zaworotko M.J. *Chem. Commun.* **2013**, *49*, 8353.
- (a) Ovsyannikov A., Ferlay S., Solovieva S.E., Antipin I.S., Konovalov A.I., Kyritsakas N., Hosseini M.W. *Inorg. Chem.* **2013**, *52*, 6776.
- (a) Ovsyannikov A., Ferlay S., Solovieva S.E., Antipin I.S., Konovalov A.I., Kyritsakas N., Hosseini M.W. *Dalton Trans.* **2014**, *43*, 158; (b) Ovsyannikov A., Ferlay S., Solovieva S.E., Antipin I.S., Konovalov A.I., Kyritsakas N., Hosseini M.W. *CrystEngComm* **2014**, *16*, 3765.
- Suffren Y., Rollet F.-G., Levasseur-Grenon O., Reber C. *Polyhedron* **2013**, *52*, 1081-1089.
- Sheldrick G.M. *Program for Crystal Structure Solution*, University of Göttingen: Göttingen, Germany, **1997**.

Received 20.07.2015

Accepted 03.08.2015